Materials Today: Proceedings 45 (2021) 7438–7443

Contents lists available at ScienceDirect

Materials Today: Proceedings

journal homepage: www.elsevier.com/locate/matpr

Control of Brushless DC motors using sensorless Back-EMF integration method

A. Attar *, J. Bouchnaif, K. Grari

Laboratory of Electrical Engineering and Maintenance, High School Of Technology, Mohammed First University, BV Mohammed VI B.P. 524, Oujda 60000, Morocco

ARTICLE INFO

Article history:
Available online 19 March 2021

Keywords:
Brushless DC motor
Sensorless
Back-EMF integration
Commutation points

ABSTRACT

This paper presents the Back Electromotive Force (Back-EMF) integration method, one of indirect Back-EMF commutation methods, used to control the sensorless Brushless Direct Current (BLDC) motor. As its name indicates this technique is based on integration of the electrical Back-EMF signal to get instantaneous information about the mechanical rotor position, correspondingly the objective of this work is to control BLDC motor without using velocity and/or position sensors, just by integration of the Back-EMF signal of the non-fed phase's to determine the position of the commutation point in order to drive the inverter. Therefore, the proposed control technique is developed using MATLAB / Simulink with Simscape library. The effectiveness of the proposed technique has been validated by simulation results

Selection and peer-review under responsibility of the scientific committee of the Fourth edition of the International Conference on Materials & Environmental Science.21 Elsevier Ltd.

1. Introduction

Brushless DC motors (BLDC) have the advantage of higher efficiency, reliability and wide speed range. Due to such individualities BLDC motor is used more and more in various industrial such as automotive, aerospace, the biomedical and robotic application [1].

Sensorless control of brushless direct-current motor (BLDC), where the BLDC motor is controlled without using position sensors, the sensorless control has great attention as research topic, according to its efficiency on reducing cost and size of the motor in same time increases the reliability of the system [2]. Most sensorless controller of BLDC motor are based on back EMF with different methods such as back EMF zero-crossing detection, third harmonic voltage integration [3], free-wheeling diodes conduction detection, and back EMF integration [4].

That paper treats the Back-EMF integration method as follows: the first section treats the model of the BLDC motor, the second section presents the sensorless Back-EMF Integration Method, the third describes the system architecture and controller design of the proposed method and last section presents simulation results of the proposed method compared with conventional position sensor method. Finally, the conclusion is given.

2. BLDC motor model

The BLDC motor has three phase symmetrical windings and rotor is made of stainless steel on which permanent magnet is mounted. Rotor current is neglected because of high resistivity of stainless steel and permanent magnet [5]. The fundamental equation governing the armature voltage equation of BLDC motor can be represented by following Fig. 1:

$$\begin{bmatrix} v_{an} \\ v_{bn} \\ v_{cn} \end{bmatrix} = \begin{bmatrix} R & 0 & 0 \\ 0 & R & 0 \\ 0 & 0 & R \end{bmatrix} \begin{bmatrix} i_a \\ i_b \\ i_c \end{bmatrix} + \begin{bmatrix} L_s - M & 0 & 0 \\ 0 & L_s - M & 0 \\ 0 & 0 & L_s - M \end{bmatrix} \frac{d}{dt} \begin{bmatrix} i_a \\ i_b \\ i_c \end{bmatrix} + \begin{bmatrix} e_a \\ e_b \\ e_c \end{bmatrix} \tag{1}$$

Where (x = a, b, c): v_{xn} represent the terminal voltage, ix represent the current of phase x, L_s represent self-inductance, M is the mutual inductance between two phases. e_x is the back-EMF voltage of the phase x: $e_a = K_e\ \omega_m\ F(\theta)$ $e_b = K_e\ \omega_m\ F(\theta\text{-}120)$ $e_c = K_e\ \omega_m\ F(\theta + 120)$ Where: K_e is the coefficient of the back-EMF, ω_m is the

* Corresponding author.
E-mail addresses: attar.abdelilah@ump.ac.ma, attar.abdelilah@gmail.com (A. Attar).

https://doi.org/10.1016/j.matpr.2021.01.861
2214-7853/
Selection and peer-review under responsibility of the scientific committee of the Fourth edition of the International Conference on Materials & Environmental Science.21 Elsevier Ltd.

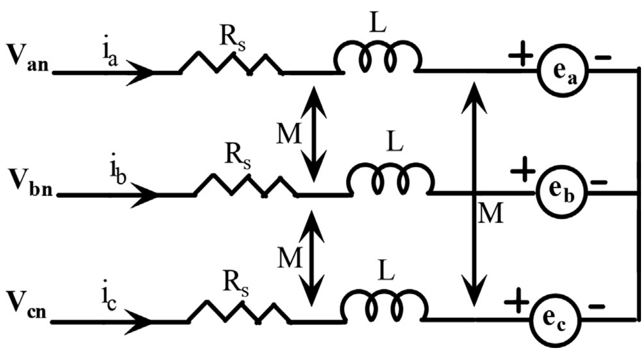

Fig. 1. Equivalent model of BLDC motor.

angular speed in rad/sec, θ is angular rotation, F(θ) is for trapezoidal back-EMF.

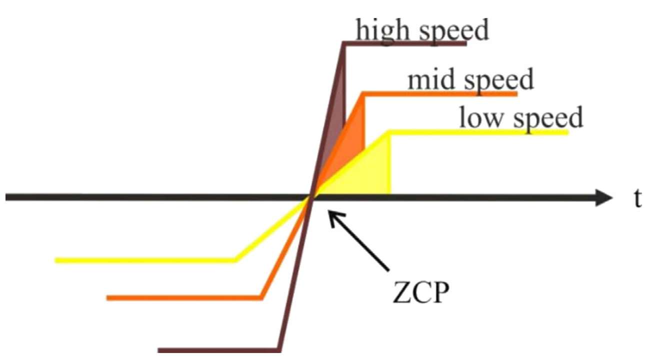

Fig. 2. Integrated areas of the back-EMF (speed-insensitive).

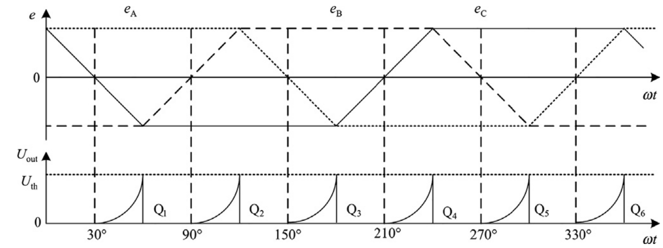

Fig. 3. Relationship between the back-EMF integration signal and the commutation instant.

3. Analysis of the proposed method

The Back-EMF Integration Method commutation instants are determined by integration of the silent phase's back-EMF (that is the unexcited phase's back-EMF). The integrated area of the of the silent phase's back-EMFs shown in Fig. 2 have approximately the same value whatever the velocity, so the principal advantage of this method is independent to velocity.

The integration starts when back-EMF of the unexcited phase crosses zero and when the integrated value reaches U_{th} the pre-defined threshold value, that moment corresponds to commutation point, and the phase current must be commutated.

Determination of the value of the threshold U_{th}:

To determinate the value of the threshold U_{th} we use the relationship between back-EMF integrated signal and the commutation instants, the back-EMF is linear, then, the function of the sloping part can be represented as is shown in Fig. 3.

Just before the point of commutation the Back-EMF is linear so we can write with the form of equation of a line:

$$e_x(t) = \pm E_0.t \tag{2}$$

The integration of the non-fed phase $e_x(t)$ starts when the back-EMF crosses zero, so the output of the integrator U are given by:

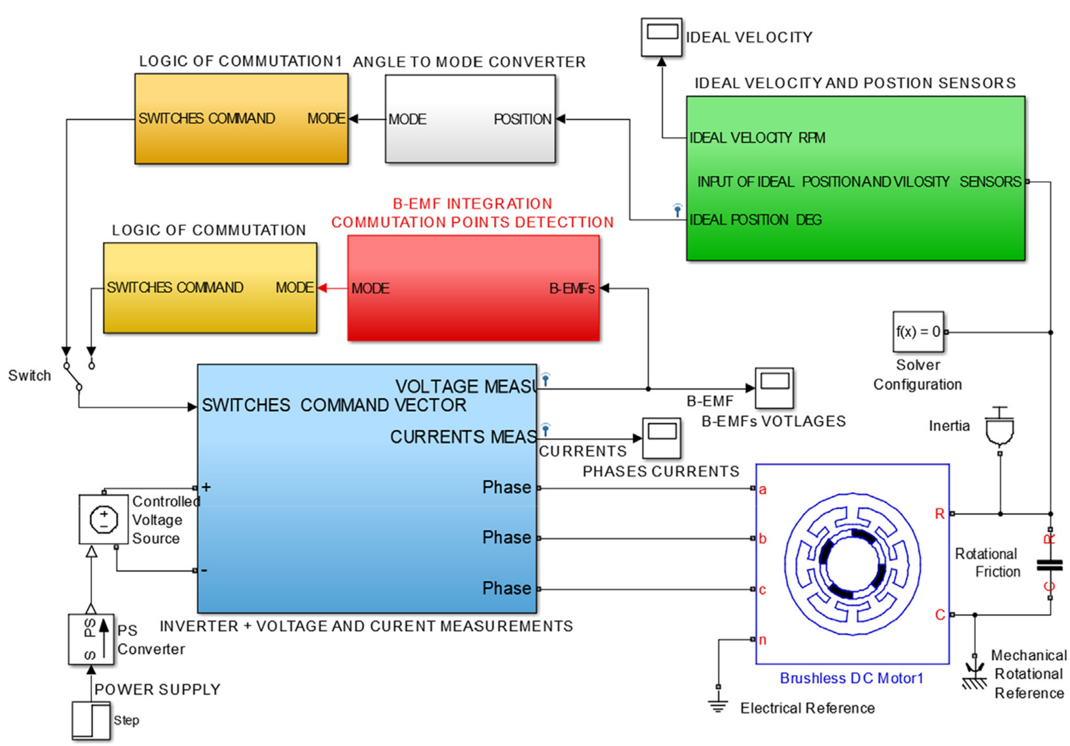

Fig. 4. BLDC motor controller scheme based on sensorless Back-EMF integration.

Table 1
The conditions of activation and deactivation Modes.

Position in degree	Modes	condition of activation	condition of deactivation	Silent phase	Switched devices
0–60	Mode 1	Threshold of Negative wave phase A is reached	Threshold of positive wave phase C is reached	B	S1 & S6
60–120	Mode 2	Threshold of positive wave phase C is reached	Threshold of Negative wave Phase B is reached	A	S3 & S6
120 to 180	Mode 3	Threshold of Negative wave Phase B is reached	Threshold of positive wave Phase A is reached	C	S2 & S3
180–240	Mode 4	Threshold of positive wave Phase A is reached	Threshold of Negative wave Phase C is reached	B	S2 & S5
240–300	Mode 5	Threshold of Negative wave Phase C is reached	Threshold of positive wave Phase B is reached	A	S4 & S5
300–360	Mode 6	Threshold of positive wave Phase B is reached	Threshold of Negative wave phase A is reached	C	S1 & S4

$$U = \left|\int_0^t \frac{e_x(t)}{k}dt\right| = \left|\frac{E_0t^2}{2k}\right| \tag{3}$$

With U is the output of the integrator and k is the gain constant of the integrator.

Therefore, the commutation instant lags the zero crossing instant of the back-EMF with a 30 degree electrical angle so the integration is from the instant 0 to t instant correspond to electrical angle $\theta_e = \frac{\pi}{6}$, so the value of threshold S_{th} is:

Table 2
BLDC motor parameters.

Stator resistance (Rs)	0.9 Ω
Stator inductance (Ls)	1.27 mH
Stator mutual inductance (Ms):	0.01 mH
Maximum permanent magnet flux linkage	50 mWb
Rotor inertia (J)	0.0001 $Kg.m^2$
Friction (B)	0.0001 N.m/(rad/s)
Number of pole pair (p)	1

$$U_{th} = \left|\frac{1}{2k}.\frac{K_e\omega}{t}t^2\right| = \left|\frac{1}{2k}.K_e\omega t\right| = \left|\frac{1}{2k}.K_e\frac{\pi}{6}\right| \tag{4}$$

where:U_{th} is the threshold, Ke is the coefficient of the back-EMF.

4. Controller design of the proposed method

The simulation of the proposed method is doing by using Simscape Simulink library, the Fig. 4 shows the global structure of the motor controller, the last one is composed by the flowing blocks: DC/AC inverter block equipped by voltage and current sensors, "Back-EMF COMMUTATION POINTS DETECTION" block implement the motor drive based on the Back-EMF integration method that block integrate the Back-EMF signal of silent phase and compared it with the threshold to give mode corresponds to the position of the rotor (Table 1), the mode gives by this block determine states of the inverter switches using the block "LOGIC OF COMMUTATION". The "ANGLE TO MODE CONVERTER" block convert the position information to the mode (sector) that block is in use to start motor, and in same time to obtain results of position sensor method to compare them with which given by the back-EMF inte-

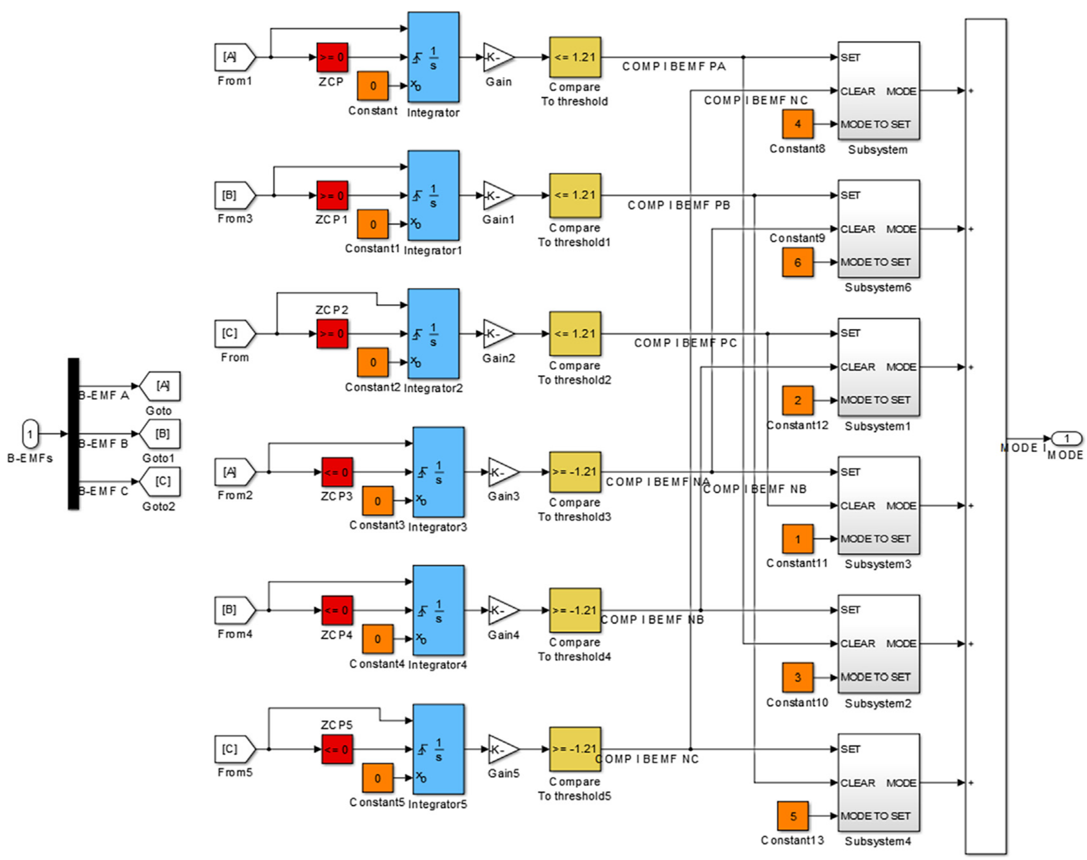

Fig. 5. Back-EMF integration commutation points detection block.

gration method. The used BLDC motor have the parameters listed in the Table 2.

To drive BLDC motor there are 6 modes, to determinate the mode and commutation point, the Fig. 5shows the block "Back-EMF integration commutation points detection" detects zero crossing from the positive and negative wave then the integrator is initialized by zero value to avoid error accumulation of the integrator the last one start integration of the current silent phase, the output of the integrator compared with the constant threshold, when the output of integrator reach that threshold the correspondent mode will be enable in the same time the precedent mode must be disable as showing in the Table 1, The integrator shall be reset after each Back-EMF zero crossing to avoid the accumulation of the error of the integrator.

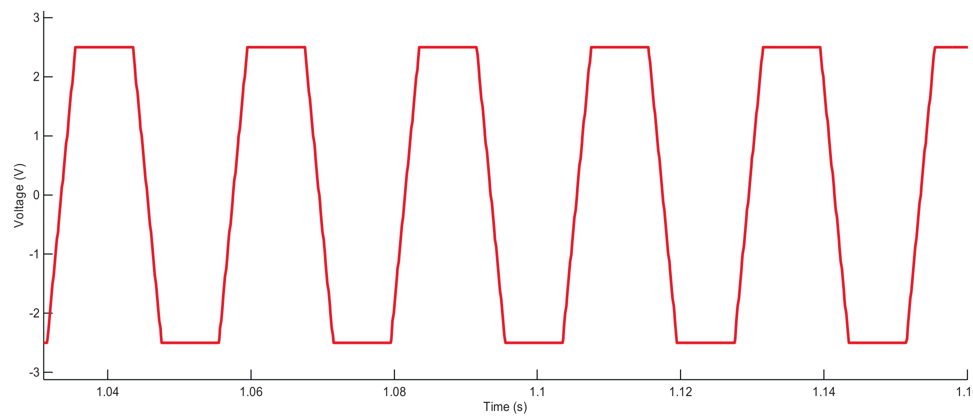

Fig. 6. Waveforms of phase A voltage given by the position sensor controller.

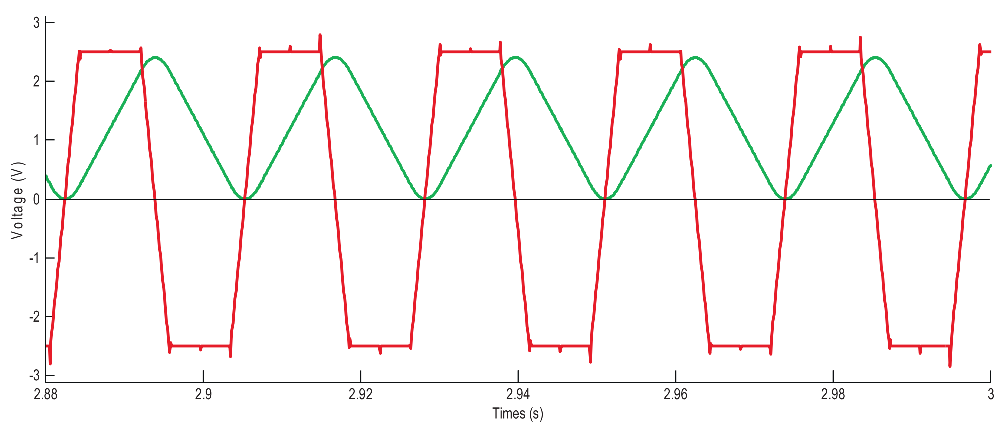

Fig. 7. Waveforms of phase A voltage and the integrate phase A voltage given by the Back-EMF integration controller.

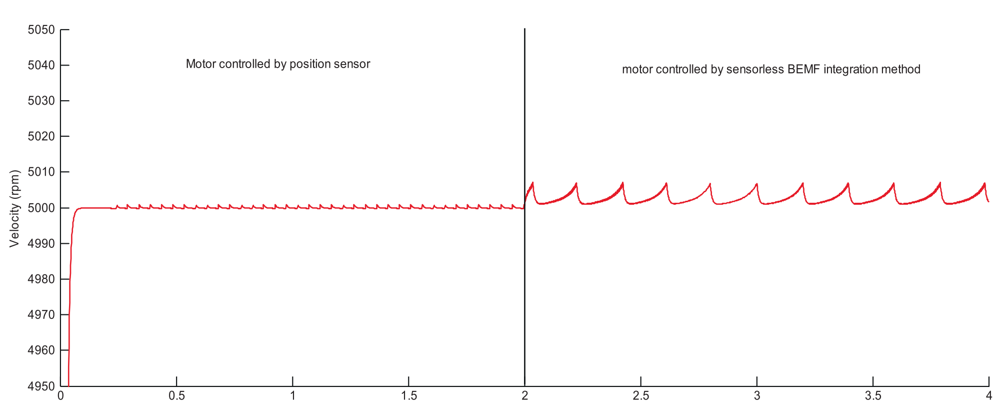

Fig. 8. Comparison of BLDC motor velocity without load for the both methods.

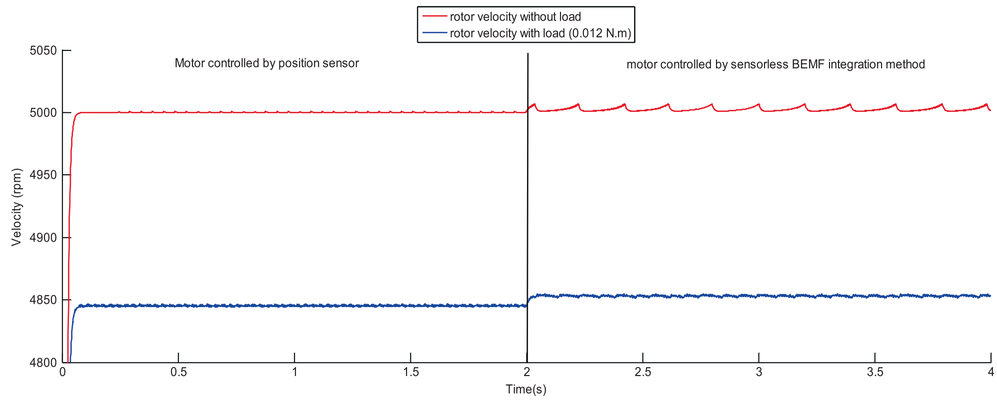

Fig. 9. Comparison of BLDC motor velocity without load for the both methods.

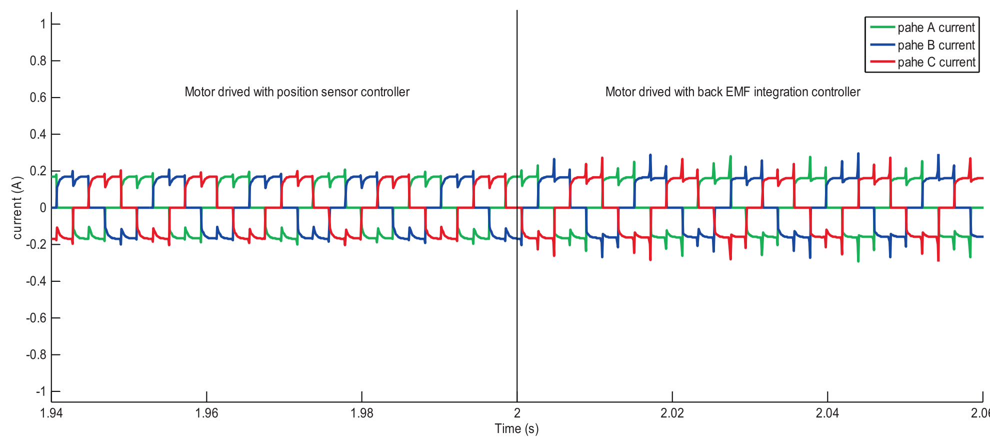

Fig. 10. MATLAB Simulation Results Showing phase current for Three Phase BLDC motor with 0.012 N.m load at speed 5000 tr.min^{-1}.

5. Results

The Back-EMF signal is captured at 2500 RPM, the form of the Back-FEM is perfectly trapezoidal in the case of control by the position sensor (Fig. 6), for the sensorless Back-EMF integration controller the form is trapezoidal but represents some switching noises (Fig. 7), they are due to poor synchronization with the commutation points.

In the Fig. 7 the green curve represents the integrate phase A voltage signal, the last one is linear in the area where the phase voltage is constant and takes proportional square of position waveform where the Back-EMF phase voltage is linear.

The both methods present ripple in the angular velocity, except that the ripple of the Back-EMF integration are a bit stronger than the sensor position method, the ripple rate is about 0.14% for the integration method versus 0.02% for the position sensor method see Fig. 8. The velocity ripple decreases when the motor is charged by a constant load of 0.012 N.m value see Fig. 9 for the proposed method.

In the BLDC motor the torque is proportional to the current so to have an idea about the generated torque we can visualize 3 phases current [6], the Fig. 10 shows the phases currents with motor under a load of 0.012 *N.m.* The both controllers give the same form of current, they have the acceptable rectangular waveform with same magnitude but for the back-EMF integration controller they have more commutation noises.

6. Conclusion

In this paper, the sensorless Back-EMF Integration method control is used to control the BLDC motor, this method is independent of the rotor velocity; the angular velocity response to a voltage step of the proposed method is satisfactory, except that it represents slight ripples which are higher than those of the control with position sensor, these ripples decrease when the motor is charged. The integration errors and threshold setup are the major causes to poor synchronisation with commutation points, that introduce current ripples, these ripples can be further minimized by adjusting the switching thresholds and/or by adding a controller.

Finally, as perspectives for this work realization of the hardware implementation, development of start-up controller, working on the self-adjustment of the switching thresholds and lastly designing on a controller that minimizes torque and speed ripples.

CRediT authorship contribution statement

A. Attar: Conceptualization, Methodology, Software, Visualization, Writing - original draft, Writing - review & editing. **J. Bouchnaif:** Methodology, Resources, Supervision, Writing - original draft, Project administration. **K. Grari:** Methodology, Resources, Writing - original draft, Project administration.

Declaration of Competing Interest

The authors declare that they have no known competing financial interests or personal relationships that could have appeared to influence the work reported in this paper.

References

[1] R.L. Valle, P.M. De Almeida, G.A. Fogli, A.A. Ferreira, P.G. Barbosa, Simple and effective digital control of a variable-speed low inductance BLDC motor drive, IEEE Access 8 (2020) 13240–13250, https://doi.org/10.1109/Access.628763910.1109/ACCESS.2020.2966437.

[2] K. Grari, J. Bouchnaif, M. Azizi, and H. Fadil, 2016. Sensorless control of switched reluctance motor with fuzzy-pi controller. 34-42.

[3] X. Song, B. Han, S. Zheng, J. Fang, High-precision Sensorless Drive for High-speed BLDC Motors based on the Virtual 3rd harmonic back-EMF. 1528–1540. 10.1109/TPEL.2017.2688478.

[4] C. Zhou, C. Xie, M. Zhang. Speed-Sensorless Control for Induction Motor Based on back-EMF Integration. 462–473. 2015. 10.1109/ICIEA.2015.7334323.

[5] M. Tariq, T.K. Bhattacharya, N. Varshney, D. Rajapan, Fast response Antiwindup PI speed controller of Brushless DC motor drive: Modeling, simulation and implementation on DSP, J. Electr. Syst. Inf. Technol. 3 (1) (2016) 1–13, https://doi.org/10.1016/j.jesit.2015.11.008.

[6] X. Yao, J. Zhao, J. Wang, S. Huang, Y. Jiang, 2019, Commutation Torque Ripple Reduction for Brushless DC Motor Based on an Auxiliary Step-Up Circuit. 7. 11. 10.1109/ACCESS.2019.2943411.